Random vibration analysis for coupled vehicle-track systems with parameter uncertainties based on hybrid pseudo excitation-polynomial chaos expansion method

P. Xiang [a]
Y. Zhao [a,*]
J.H. Lin [a]
D. Kennedy [b]
F.W. Williams [b]

[a]State Key Laboratory of Structural Analysis for Industrial Equipment, Faculty of Vehicle Engineering and Mechanics, Dalian University of Technology, Dalian 116023, PR China
[b]Cardiff School of Engineering, Cardiff University, Cardiff CF24 3AA, Wales, UK

[*]Corresponding author email: yzhao@dlut.edu.cn

Abstract

This paper proposes a new random vibration-based assessment method for coupled vehicle-track systems with uncertain parameters when subjected to random track irregularity. The vehicle system is simplified to a spring-mass-damper model defined by physical coordinates, while the uncertainties of the vehicle parameters are described as bounded random variables. The track is regarded as an infinite periodic structure, and the dynamic equations of the coupled vehicle-track system, under mixed physical coordinates and symplectic dual coordinates, are established through wheel-rail coupling relationships. The random track irregularities at the wheel-rail contact points are converted to a series of deterministic harmonic excitations with phase lag by using the pseudo excitation method (PEM). Based on the polynomial chaos expansion of the pseudo response, a new chaos expanded pseudo equation is derived, leading to the combined hybrid pseudo excitation method - polynomial chaos expansion (PEM-PCE) method which can efficiently assess the impact of uncertainty propagation on the random vibration analysis. The proposed method is compared with Monte Carlo simulations and good agreement was achieved. It is an effective means for random vibration analysis of uncertain coupled vehicle-track system and has good engineering practicality.

Keywords

Uncertainty; Vehicle-track coupled systems; Polynomial chaos expansion; Pseudo excitation method; Symplectic

1 Introduction

There are many uncertainties in practical train structures due to inaccurate processing and manufacture and so a deterministic model is only an approximation of the real structure. In order to achieve more reliable predictions for the dynamic behavior of trains and their relationship to the railway lines, it is necessary to consider the system uncertainties and to develop a method for predicting their propagation in the coupled system. Over the last decade, this topic has received increasing attention. (D'Aveni *et al.*, 1996) established an analytical method for a simply supported beam with uncertain damping ratio and elastic modulus subjected to a deterministic excitation. Their work included the expansion of the uncertain quantities by a perturbation technique, together with the evaluation of the transition matrix of the stochastic system. (Muscolino *et al.*, 2002) concentrated on the problem of calculating the random response of a distributed parameter system subjected to a moving oscillator with uncertain mass, velocity and acceleration. (Chang *et al.*, 2006) investigated the dynamic response of a fixed-fixed beam with an internal hinge on an elastic foundation when it was subjected to an uncertain moving oscillator (*e.g.* random mass, stiffness, damping and acceleration) and a set of approximate governing equations of motion were developed using modal analysis and Galerkin's method. They subsequently adopted an improved perturbation technique in order to evaluate the statistical responses of the beam. (Gladysz and Śniady, 2009) carried out a power spectral analysis for a beam with uncertain parameters subjected to a moving force that was assumed to be modeled as a filtered Poisson process, on the assumption that the natural frequencies of the structure were uncertain and were modeled by fuzzy numbers, random variables or fuzzy random variables. General solutions for the spectral density were obtained using a modal dynamic influence function. (Wu and Law, 2010; 2011) investigated the interaction of uncertain vehicle-bridge systems, with the bridge modeled as a simply supported Euler-Bernoulli beam with non-Gaussian material parameters, while the vehicle was modeled by a four degree of freedom mass-spring system. The road surface roughness was assumed to be a Gaussian random process; the non-Gaussian uncertainty was handled by means of the Spectral Stochastic Finite Element (SSFE) and the equations of the vehicle-bridge system were solved using the Newmark method, with suggested order for both Polynomial Chaos and threshold for truncation in the Karhunen–Loève expansion.

The polynomial chaos expansion (PCE) method, as a non-sampling method, has been widely used to investigate various uncertain problems. This method was first presented by (Wiener, 1938) based on homogeneous chaos theory. According to the theorem of (Cameron and Martin, 1947), the homogeneous chaos expansion converges to any stochastic process with finite second-order moments, which provides a means for Hermitian polynomials to represent the stochastic process. In the field of structural dynamics, (Ghanem *et al*., 1991) presented a spectrum approach for solution of stochastic mechanics by combining Hermitian chaos and finite element method. In a series of subsequent developments, (Ghanem and Kruger, 1996; Ghanem and Red-Horse, 1999) have further promoted research in uncertain structural dynamics. Hermitian polynomials are aimed at Gaussian distribution parameters and are subject to some limitations in applications. Therefore, (Xiu and Karniadakis, 2002; 2010) developed the generalized polynomial chaos (gPC) method (*i.e.* the Wiener-Askey scheme), by means of which the optimal convergence polynomials were given according to different probability distributions, and an efficient stochastic collocation method was developed to overcome the difficulty caused by multiple variables. In the field of vehicle dynamics, (Kewlani *et al.*, 2012) investigated the random dynamic behavior of 3-D vehicles

moving on an uneven surface, establishing an evaluation method for system responses based on the gPC method combined with the efficient collocation method (ECM). The experimental results and numerical simulation well justified this approach.

The pseudo excitation method (PEM) is a well-established algorithm for analyzing the responses of deterministic systems under stationary or non-stationary random excitations (Lin *et al*., 1992; 2001; 2011; 2014). Because of its simplicity and high efficiency, PEM has been widely used in many engineering fields (Caprani, 2014; Lin *et al.*, 2014; Yu, 2010; Zhang and Xu, 1999; Zhang *et al.*, 2010). The problem under consideration in this paper is a double-random problem, in that it deals with a system with uncertainty subjected to random excitations. The parameters of the coupled vehicle-track system are uncertain, and are characterized as random variables with an arch probability distribution. Therefore Chebyshev polynomials are the optimal selection for the orthogonal basis function of which the weight function is equal to the probability density function (PDF) of the random variable. The track irregularities, as the excitations acting to the system, are regarded as the spatial random process. The uncertainty of the structural parameters and the randomness of the excitations are handled in different ways by the proposed PEM-PCE method. By using PEM in this paper, the track irregularities are converted to harmonic pseudo excitations and then only the harmonic pseudo governing equation needs to be solved. The Galerkin method is used to produce the polynomial chaos expansion coefficients of the pseudo responses. To reduce the dimension of the governing equation, the state equation of a typical substructure is established in the Hamiltonian space using the symplectic method according to the periodicity of the track substructures, so that only typical sub-structures need be taken into account in the numerical computations.

In this paper we establish an effective assessment method of random vibration analysis for uncertain coupled vehicle-track systems subjected to track irregularity. In section 2, the principle and application for uncertain system of PEM was introduced. In section 3, the governing equation of coupled vehicle-track systems under mixed physical coordinates and symplectic dual coordinates were established through wheel-rail coupling relationships. In section 4, a hybrid pseudo excitation - polynomial chaos expansion method (PEM-PCE) is proposed to solve the random vibration problem of uncertain structures. In the numerical example, a 10 degree of freedom rigid body vehicle model is adopted. The random vibration behavior of the coupled system due to different parameters at different velocities is discussed. Comparison with the direct Monte Carlo simulation shows that the proposed method significantly improves efficiency while preserving very high accuracy. Hence the results show that the proposed method is very promising in both the accuracy and efficiency.

2 Pseudo excitation method

2.1 Pseudo excitation method for deterministic systems

The equation of motion of a linear deterministic system subjected to a stationary random excitation $\mathbf{p}(t)$ is

$$\mathbf{m}\ddot{\mathbf{x}}(t) + \mathbf{c}\dot{\mathbf{x}}(t) + \mathbf{k}\mathbf{x}(\boldsymbol{t}) = \mathbf{p}(\boldsymbol{t}) \tag{2.1}$$

The form in the frequency domain is

$$[(\mathbf{k} - \omega^2\mathbf{m}) + \mathrm{i}\omega\mathbf{c}]\mathbf{X}(\mathrm{i}\omega) = \mathbf{P}(\mathrm{i}\omega) \tag{2.2}$$

where $\mathbf{X}(\mathrm{i}\omega)$ and $\mathbf{P}(\mathrm{i}\omega)$ are the Fourier transforms of $\mathbf{x}(t)$ and $\mathbf{p}(t)$, respectively; i is the

imaginary unit.

The response can be expressed as

$$\mathbf{X}(\mathrm{i}\omega) = \mathbf{H}(\mathrm{i}\omega)\mathbf{P}(\mathrm{i}\omega) \tag{2.3}$$

where $\mathbf{H}(\mathrm{i}\omega) = [\mathbf{k} - \omega^2\mathbf{m} + \mathrm{i}\omega\mathbf{c}]^{-1}$is the frequency response matrix.

According to conventional random vibration theory, the power spectrum density function of response $\mathbf{S}_x(\mathrm{i}\omega)$ can be obtained (Clough and Penzien, 1975) from

$$\mathbf{S}_{\boldsymbol{x}}(\mathrm{i}\omega) = \mathbf{H}(\mathrm{i}\omega)^*\mathbf{S}_p(\mathrm{i}\omega)\mathbf{H}(\mathrm{i}\omega)^{\mathrm{T}} \tag{2.4}$$

where the asterisk denotes complex conjugate, the superscript T denotes transpose; $\mathbf{S}_p(\mathrm{i}\omega)$ is the power spectral density (PSD) matrix of random excitation $\mathbf{p}(t)$.

For complicated FEM systems, the computational effort is often unacceptable. In order to overcome this difficulty, the following pseudo-excitation method (PEM) has been proved very efficient.

Note that $\mathbf{S}_p(\mathrm{i}\omega)$ is an n_s order Hermitian matrix with rank q, which can be decomposed as (De Rosa *et al.*, 2015，Lin *et al.*, 2014)

$$\mathbf{S}_p(\mathrm{i}\omega) = \sum_{d=1}^{q} \lambda_d \boldsymbol{\psi}_d^* \boldsymbol{\psi}_d^{\mathrm{T}} \quad (q \le n_s) \tag{2.5}$$

where λ_d and $\boldsymbol{\psi}_d$ are the eigenvalue and corresponding eigenvector of $\mathbf{S}_p(\mathrm{i}\omega)$.

Constructing the pseudo excitations

$$\tilde{\mathrm{P}}_{\mathrm{d}}(\mathrm{i}\omega) = \sqrt{\lambda_{\mathrm{d}}}\psi_{\mathrm{d}}\mathrm{e}^{\mathrm{i}\omega\mathrm{t}} \ \ (\mathrm{d} = 1,2,\dots,\mathrm{q}) \tag{2.6}$$

Substitute (2.6) for $\widetilde{\mathbf{P}}(t)$ in Equation (2.3)

$$\widetilde{\mathbf{X}}_d(\mathrm{i}\omega) = \mathbf{H}(\mathrm{i}\omega)\widetilde{\mathbf{P}}_d(\mathrm{i}\omega) \tag{2.7}$$

where $\widetilde{\mathbf{X}}_d(i\omega)$ is called pseudo response. Clearly,

$$\widetilde{\mathbf{X}}_d^*\widetilde{\mathbf{X}}_d^{\mathrm{T}} = \mathbf{H}(\mathrm{i}\omega)^*\lambda_d\boldsymbol{\psi}_d^*\boldsymbol{\psi}_d^{\mathrm{T}}\mathbf{H}(\mathrm{i}\omega)^{\mathrm{T}} \tag{2.8}$$

According to Equation (2.4) and (2.5), one obtains

$$\sum_{d=1}^{q} \widetilde{\mathbf{X}}_d^*\widetilde{\mathbf{X}}_d^{\mathrm{T}} = \mathbf{H}(\mathrm{i}\omega)^*\mathbf{S}_p(\mathrm{i}\omega)\mathbf{H}(\mathrm{i}\omega)^{\mathrm{T}} = \mathbf{S}_x(\mathrm{i}\omega) \tag{2.9}$$

As a special and important case, when the random excitations at different points are fully coherent, the PSD matrix can be decomposed as the product of two vectors, *i.e.* only one λ_d in equation (2.5) is non-zero, and so $\mathbf{S}_p(\mathrm{i}\omega)$ has the form

$$\mathbf{S}_p(\mathrm{i}\omega) = \begin{bmatrix} a_1^2 & a_1a_2e^{\mathrm{i}\omega(t_1-t_2)} & \dots & a_1a_{n_s}e^{\mathrm{i}\omega(t_1-t_{n_s})} \\ a_2a_1e^{\mathrm{i}\omega(t_2-t_1)} & a_2^2 & \dots & a_2a_{n_s}e^{\mathrm{i}\omega(t_2-t_{n_s})} \\ \vdots & \vdots & \ddots & \vdots \\ a_{n_s}a_1e^{\mathrm{i}\omega(t_{n_s}-t_1)} & a_{n_s}a_2e^{\mathrm{i}\omega(t_{n_s}-t_2)} & \dots & a_{n_s}^2 \end{bmatrix} S_p(\omega) \tag{2.10}$$

where $a_i\ (i = 1,2,\dots,n_s)$ represents the strengths at different excitation points, and the pseudo excitation can be written as

$$\widetilde{\mathbf{P}}(\mathrm{i}\omega) = \mathbf{V}\sqrt{S_p}e^{\mathrm{i}\omega t} \tag{2.11}$$

where $\mathbf{V} = \left\{a_1e^{-\mathrm{i}\omega t_1}, a_2e^{-\mathrm{i}\omega t_2}, \dots, a_{n_s}e^{-\mathrm{i}\omega t_{n_s}}\right\}^{\mathrm{T}}$.

So the pseudo response is

$$\widetilde{\mathbf{X}}(\mathrm{i}\omega) = \mathbf{H}(\mathrm{i}\omega)\mathbf{V}\sqrt{S_p}e^{\mathrm{i}\omega t} \tag{2.12}$$

The PSD of $\mathbf{x}$ can be obtained from

$$\mathbf{S}_x(\mathrm{i}\omega) = \widetilde{\mathbf{X}}^*\widetilde{\mathbf{X}}^{\mathrm{T}} \tag{2.13}$$

The above are the basic formulae of the PEM for deterministic systems subjected to stationary random excitations, which are exactly equivalent to Equation (2.4). However the computation is much more efficient.

2.2 Pseudo excitation method for uncertain system

It is assumed that the randomness of the external load is independent of the uncertainty of the parameters, and that the random load is fully characterized by the PSD. So the construction of pseudo excitation for uncertain system is the same as that for deterministic system, *i.e.* as derived in Section 2.1.

In the framework of the PEM, the governing equation of the uncertain system is expressed as

$$[\mathbf{k}(\boldsymbol{\alpha}) - \omega^2\mathbf{m}(\boldsymbol{\alpha}) + \mathrm{i}\omega\mathbf{c}(\boldsymbol{\alpha})]\widetilde{\mathbf{X}}(\mathrm{i}\omega) = \widetilde{\mathbf{P}}(\mathrm{i}\omega) \tag{2.14}$$

The uncertainties of parameters are characterized in the frequency-response matrix, $\mathbf{H}(\mathrm{i}\omega, \boldsymbol{\alpha})$ and the pseudo response is

$$\widetilde{\mathbf{X}}(\mathrm{i}\omega, \boldsymbol{\alpha}) = \mathbf{H}(\mathrm{i}\omega, \boldsymbol{\alpha})\widetilde{\mathbf{P}}(\mathrm{i}\omega) \tag{2.15}$$

Let $\{\phi_k(\boldsymbol{\alpha})\}_{k=0}^{\infty} \subset \mathbb{P}$ be an orthogonal polynomial space. The pseudo response can be expanded in terms of the basis functions

$$\widetilde{\mathbf{X}}(\mathrm{i}\omega, \boldsymbol{\alpha}) = \boldsymbol{\phi}(\boldsymbol{\alpha})\hat{\mathbf{x}}(\mathrm{i}\omega) \tag{2.16}$$

where $\hat{\mathbf{x}}(\mathrm{i}\omega)$ are the coefficients of the basis functions, of which the solution will be derived in Section 4.3.

By using PEM, the PSD can be expressed as

$$\mathbf{S}_x(\mathrm{i}\omega, \boldsymbol{\alpha}) = \widetilde{\mathbf{X}}(\mathrm{i}\omega, \boldsymbol{\alpha})^*\widetilde{\mathbf{X}}(\mathrm{i}\omega, \boldsymbol{\alpha})^{\mathrm{T}} = \boldsymbol{\phi}(\boldsymbol{\alpha})^*\hat{\mathbf{x}}(\mathrm{i}\omega)^*\hat{\mathbf{x}}(\mathrm{i}\omega)^{\mathrm{T}}\boldsymbol{\phi}(\boldsymbol{\alpha})^{\mathrm{T}} \tag{2.17}$$

3 Governing equation

The model used for the coupled vehicle-track system is shown in Figure 1 which shows: the velocity v (from left to right); a multi-rigid model for the two-suspension structures of the vehicle, the mass of the carriage M_c and its moment of inertia J_c; the half span of the bogie spacing l_c ; the mass of the bogie M_t and its moment of inertia J_t; the half span of the wheel spacing l_t; the mass of the wheels M_w; the primary suspension stiffness and damping k_t^i and c_t^i $(i = 1,2,3,4)$; the secondary suspension stiffness and damping k_c^i and c_c^i $(i = 1,2)$. Figure 1 also shows how the track is regarded as a three layer structure, comprising the rail, sleepers and ballast, with the rail modeled as a single Bernoulli–Euler beam with bending rigidity EI and uniform mass / unit length m_r; sleeper and ballast masses of m_s and m_b; rail pad, ballast and subgrade stiffnesses of k_p, k_b and k_f; and corresponding damping of c_p, c_b and c_f. A linearized spring of stiffness $k_h = 1.5P_0^{1/3}/\mathrm{G}$ connects the wheels to the rail, where P_0 and G, respectively, represent the static interaction and a connection constant between the wheels and rail (Thompson, 1993).

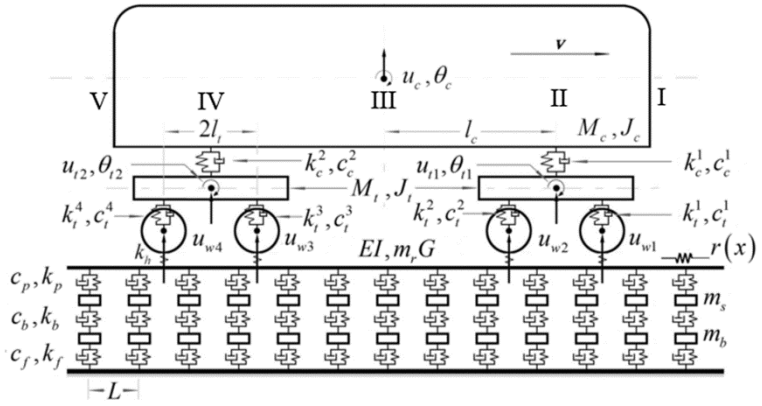

Figure 1: The coupled vehicle-track systems.

3.1 Equation of motion of the vehicle

There are ten degrees of freedom on the model, see Figure 1. These are the vertical and rotational motion of the carriage $(u_c, \theta_c)$and of its two identical bogies,$(u_{t1}, \theta_{t1}, u_{t2}, \theta_{t2})$ plus the vertical motions of the four rigid wheels $(u_{w1}, u_{w2}, u_{w3}, u_{w4})$. The degree of freedom vector used is

$$\mathbf{u}_v = \{u_c, \theta_c, u_{t1}, \theta_{t1}, u_{t2}, \theta_{t2}, u_{w1}, u_{w2}, u_{w3}, u_{w4}\}^{\mathrm{T}} \tag{3.1}$$

Denoting the kth component of vector $\mathbf{u}_v$ by u_k, the equation of motion of the vehicle, using the Lagrange equation, is

$$\frac{d}{dt}\left(\frac{\partial T}{\partial \dot{q}_k}\right) - \frac{\partial T}{\partial q_k} + \frac{\partial V}{\partial \dot{q}_k} + \frac{\partial Q}{\partial \dot{q}_k} = 0 \tag{3.2}$$

where T, V and Q respectively denote kinetic energy, elastic potential energy and damping dissipated energy.

Substituting the energy represented by $\mathbf{u}_v$ into Equation (3.2) gives the equation of motion of the vehicle as

$$\mathbf{M}_v\ddot{\mathbf{u}}_v + \mathbf{C}_v\dot{\mathbf{u}}_v + \mathbf{K}_v\mathbf{u}_v = \tilde{\mathbf{f}}_v \tag{3.3}$$

where $\mathbf{K}_v$, $\mathbf{M}_v$ and $\mathbf{C}_v$ are the stiffness, mass and damping matrices of the vehicle and $\tilde{\mathbf{f}}_v$ is the pseudo excitation caused by track irregularity whose specific form will be given by the wheel rail relationships in a later section.

3.2 Equation of motion of the track

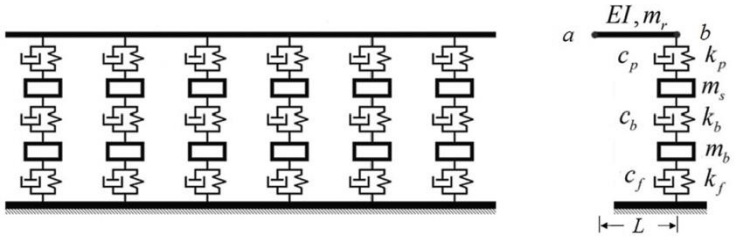

Figure 2: The periodic arrangement of the elastic track and a typical substructure.

The track is regarded as an infinitely long periodic chain in which the substructure consists of the rail between adjacent sleepers, a sleeper and the associated ballast, as shown in Figure 2. The equation of motion in the frequency domain of each substructure can then be expressed as

$$(\mathbf{K} + i\omega\mathbf{C} - \omega^2\mathbf{M})\begin{Bmatrix}\mathbf{u}_i^0\\ \mathbf{u}_a^0\\ \mathbf{u}_b^0\end{Bmatrix} = \begin{bmatrix}\mathbf{G}_{ii}^0 & \mathbf{G}_{ia}^0 & \mathbf{G}_{ib}^0\\ \mathbf{G}_{ai}^0 & \mathbf{G}_{aa}^0 & \mathbf{G}_{ab}^0\\ \mathbf{G}_{bi}^0 & \mathbf{G}_{ba}^0 & \mathbf{G}_{bb}^0\end{bmatrix}\begin{Bmatrix}\mathbf{u}_i^0\\ \mathbf{u}_a^0\\ \mathbf{u}_b^0\end{Bmatrix} = \begin{Bmatrix}\mathbf{p}_i^0\\ \mathbf{p}_a^0\\ \mathbf{p}_b^0\end{Bmatrix} \tag{3.4}$$

Here $\mathbf{M}$, $\mathbf{K}$ and $\mathbf{C}$ are the mass, stiffness and damping matrices of the substructure; $\mathbf{u}_a^0$ and $\mathbf{u}_b^0$ are the displacement vectors at the left and right side interfaces; $\mathbf{u}_i^0$ is the internal displacement vector; and $\mathbf{p}_a^0$, $\mathbf{p}_b^0$ and $\mathbf{p}_i^0$ are the corresponding nodal force vectors.

Eliminating the internal displacement vector $\mathbf{u}_i^0$, Equation (3.4) can be described by the interface displacement vectors as

$$\begin{bmatrix}\mathbf{G}_{aa} + \mathbf{P}_\beta & \mathbf{G}_{ab}\\ \mathbf{G}_{ba} & \mathbf{G}_{bb} + \mathbf{P}_\alpha\end{bmatrix}\begin{Bmatrix}\mathbf{u}_a\\ \mathbf{u}_b\end{Bmatrix} = \begin{Bmatrix}\mathbf{p}_a^*\\ \mathbf{p}_b^*\end{Bmatrix} \tag{3.5}$$

where

$$\mathbf{G}_{aa}=\mathbf{G}_{aa}^{0}-\mathbf{G}_{ai}^{0}\left[\mathbf{G}_{ii}^{0}\right]^{-1}\mathbf{G}_{ia}^{0}\quad \mathbf{G}_{ab}=\mathbf{G}_{ab}^{0}-\mathbf{G}_{ai}^{0}\left[\mathbf{G}_{ii}^{0}\right]^{-1}\mathbf{G}_{ib}^{0}$$

$$\mathbf{G}_{ba}=[\mathbf{G}_{ab}]^{\mathrm{T}}\qquad \mathbf{G}_{bb}=\mathbf{G}_{bb}^{0}-\mathbf{G}_{bi}^{0}\left[\mathbf{G}_{ii}^{0}\right]^{-1}\mathbf{G}_{ib}^{0}$$

$$\mathbf{p}_{a}^{*}=\mathbf{p}_{ae}-\mathbf{G}_{ai}^{0}\left[\mathbf{G}_{ii}^{0}\right]^{-1}\mathbf{p}_{ie}\quad \mathbf{p}_{b}^{*}=\mathbf{p}_{be}-\mathbf{G}_{bi}^{0}\left[\mathbf{G}_{ii}^{0}\right]^{-1}\mathbf{p}_{ie}$$

Here, $\mathbf{P}_{\alpha}$ and $\mathbf{P}_{\beta}$ are the dynamic stiffness matrices at the two interfaces of the substructure, and $\mathbf{p}_{ae}$, $\mathbf{p}_{be}$ and $\mathbf{p}_{ie}$ are the actual external loads.

Considering the displacement and force as the state vector, when the substructure has no external loads (*i.e.* $\mathbf{p}_{ae}=\mathbf{p}_{be}=\mathbf{p}_{ie}=\mathbf{0}$) Equation (3.5) has the following form in state space

$$\begin{Bmatrix}\mathbf{u}_{b}\\ \mathbf{p}_{b}\end{Bmatrix}=\begin{bmatrix}\mathbf{S}_{aa} & \mathbf{S}_{ab}\\ \mathbf{S}_{ba} & \mathbf{S}_{bb}\end{bmatrix}\begin{Bmatrix}\mathbf{u}_{a}\\ \mathbf{p}_{a}\end{Bmatrix} \tag{3.6}$$

where

$$\mathbf{S}_{aa}=-[\mathbf{G}_{ab}]^{-1}\mathbf{G}_{aa}\quad \mathbf{S}_{ab}=[\mathbf{G}_{ab}]^{-1}$$
$$\mathbf{S}_{ba}=-\mathbf{G}_{ba}+\mathbf{G}_{bb}[\mathbf{G}_{ab}]^{-1}\mathbf{G}_{aa}\qquad \mathbf{S}_{bb}=-\mathbf{G}_{bb}[\mathbf{G}_{ab}]^{-1}$$
$$\mathbf{p}_{a}=-\mathbf{P}_{\beta}\mathbf{u}_{a}\qquad \mathbf{p}_{b}=-\mathbf{P}_{\boldsymbol{\alpha}}\mathbf{u}_{\boldsymbol{b}}$$

Equation (3.6) can be denoted as

$$\mathbf{y}_{b}=\mathbf{S}\mathbf{y}_{a} \tag{3.7}$$

It can be verified that $\mathbf{S}^{-\mathrm{T}}=\mathbf{J}\mathbf{S}\mathbf{J}^{-1}$ or $\mathbf{S}^{\mathrm{T}}\mathbf{J}\mathbf{S}=\mathbf{J}$, where $\mathbf{S}$ is a symplectic matrix which satisfies the symplectic orthogonality relationships and

$$\mathbf{J}=\begin{bmatrix}\mathbf{0} & \mathbf{I}_{n_0}\\ -\mathbf{I}_{n_0} & \mathbf{0}\end{bmatrix} \tag{3.8}$$

where $\mathbf{I}_{n_0}$ is an n_0 order identity matrix; n_0 is the number of degrees of freedom of the interface.

It is known from symplectic mathematical theory that if $|\mu_i|\le 1$ is an eigenvalue of $\mathbf{S}$, then so is $\mu_{n_0+i}=1/\mu_i$ (Lin *et al*., 1995). Assume now that $\mathbf{S}$ has $2n_0$ eigenvalues and let them be separated into the following two groups

$$\begin{cases}\mu_i & i=1,2,\dots,n_0 \quad |\mu_i|\le 1\\ \mu_{n_0+i}=1/\mu_i & i=1,2,\dots,n_0 \quad |\mu_i|\ge 1\end{cases} \tag{3.9}$$

The corresponding eigenvectors can then be used to constitute the matrix

$$\boldsymbol{\Theta}=\{\boldsymbol{\psi}_1,\boldsymbol{\psi}_2,\dots,\boldsymbol{\psi}_{2n_0}\}=\begin{bmatrix}\mathbf{X}_a & \mathbf{X}_b\\ \mathbf{N}_a & \mathbf{N}_b\end{bmatrix} \tag{3.10}$$

The state vector $\mathbf{y}$ can be expanded in terms of the eigenvectors as

$$\mathbf{y}=\Sigma_{i=1}^{n_0}(a_i\boldsymbol{\psi}_i+b_i\boldsymbol{\psi}_{n+i}) \tag{3.11}$$

The coefficients a_i and b_i are rewritten in vector forms $\mathbf{a}$ and $\mathbf{b}$.

When the substructure is subjected to a harmonic load, the state vector of the interfaces between substructures can be obtained by harmonic wave propagation theory as

$$\begin{cases}\mathbf{y}_{kr}=\begin{bmatrix}\mathbf{X}_a\\ \mathbf{N}_a\end{bmatrix}\boldsymbol{\mu}^{k}\mathbf{a} & k\ge 0 \text{ (go right)}\\ \mathbf{y}_{kl}=\begin{bmatrix}\mathbf{X}_b\\ \mathbf{N}_b\end{bmatrix}\boldsymbol{\mu}^{-k}\mathbf{b} & k\le 0 \text{ (go left)}\end{cases} \tag{3.12}$$

Only when $|\mu_i|=1$ can the harmonic wave be propagated in the entire substructure chain, and it is called a pass wave. The remaining harmonic waves decay rapidly away in the propagation, and are called obstructed waves.

When the substructure is subjected to a harmonic excitation, *i.e.* $k = 0$in Equation (3.12).

$$\begin{Bmatrix}\mathbf{u}_a\\ \mathbf{u}_b\end{Bmatrix} = \begin{bmatrix}\mathbf{X}_b & \mathbf{0}\\ \mathbf{0} & \mathbf{X}_a\end{bmatrix}\begin{Bmatrix}\mathbf{b}\\ \mathbf{a}\end{Bmatrix} \tag{3.13}$$

Thus the interface stiffness matrices in Equation (3.5) can be written as

$$\mathbf{P}_\alpha = \mathbf{N}_a\mathbf{X}_a^{-1} \quad \mathbf{P}_\beta = -\mathbf{N}_b\mathbf{X}_b^{-1} \tag{3.14}$$

Substituting Equation (3.13) into Equation (3.5) yields the equation of motion denoted by the symplectic modal coordinate $\{\mathbf{b}^{\mathrm{T}}, \mathbf{a}^{\mathrm{T}}\}^{\mathrm{T}}$ as

$$\begin{bmatrix}\mathbf{G}_{aa}+\mathbf{P}_\beta & \mathbf{G}_{ab}\\ \mathbf{G}_{ba} & \mathbf{G}_{\boldsymbol{bb}}+\mathbf{P}_\alpha\end{bmatrix}\begin{bmatrix}\mathbf{X}_b & \mathbf{0}\\ \mathbf{0} & \mathbf{X}_a\end{bmatrix}\begin{Bmatrix}\mathbf{b}\\ \mathbf{a}\end{Bmatrix} = \begin{Bmatrix}\mathbf{p}_{\mathrm{a}}^*\\ \mathbf{p}_{\mathrm{b}}^*\end{Bmatrix} \tag{3.15}$$

3.3 Mixed coordinate equations of motion of the coupled vehicle-track

In the equation of motion of the vehicle, *i.e.* Equation (3.3), $\tilde{\mathbf{f}}_{\boldsymbol{v}}$ can be written as

$$\tilde{\mathbf{f}}_{\boldsymbol{v}} = \{0_{6\times1} \quad f_1 \quad f_2 \quad f_3 \quad f_4\}^{\mathrm{T}} \tag{3.16}$$

For the ith substructure subjected to the wheel-rail force, decomposing the force to the interfaces, Equation (3.15) can be expressed as

$$\begin{bmatrix}\left(\mathbf{G}_{aa}+\mathbf{P}_\beta\right)\mathbf{X}_b & \mathbf{G}_{ab}\mathbf{X}_a\\ \mathbf{G}_{ba}\mathbf{X}_b & (\mathbf{G}_{\boldsymbol{bb}}+\mathbf{P}_\alpha)\mathbf{X}_a\end{bmatrix}\begin{Bmatrix}\mathbf{b}_i\\ \mathbf{a}_i\end{Bmatrix} = -\mathbf{N}(\xi_i)f_i \quad (i = 1,2,3,4) \tag{3.17}$$

where $\mathbf{N}(\xi)$ is the shape function vector of the Bernoulli-Euler beam element, and ξ_i is the local coordinate of the position of the ith wheel-rail force.

Based on the Hertz formula, the interaction between wheels and rails is modeled as a linear spring connection of stiffness k_h. Hence the wheel-rail force of the ith substructure can be expressed as

$$f_i = k_h\left(u_{t_i} - u_{w_i} - r_i\right) \quad i = 1,2,3,4 \tag{3.18}$$

where u_{t_i} is the displacement of the pair of rails at the ith contact point, $u_{w_i}$is the displacement and r_i is the track irregularity.

Based on the eigenvector expansion method, the left- and right-hand displacement vectors of the i th substructure, $\mathbf{u}_{a,i}$ and $\mathbf{u}_{b,i}$, can be obtained as the sum of the responses caused by each of the four wheel–rail forces, *i.e.*

$$\mathbf{u}_{a,i} = \Sigma_j^4\mathbf{u}_{a,ji}\,,\ \mathbf{u}_{b,i} = \Sigma_j^4\mathbf{u}_{b,ji} \tag{3.19}$$

where $\mathbf{u}_{a,ji}$ and $\mathbf{u}_{a,ji}$ are the left- and right-hand displacement vectors of the ith substructure caused by the responses of the jth substructure.

For the displacement of the pair of rails at the contact point, such as the displacement of the ith substructure, the contact point u_{t_i} can be obtained from

$$u_{t_i} = \mathbf{N}^{\mathrm{T}}(\xi_i)\begin{Bmatrix}\mathbf{u}_{a,i}\\ \mathbf{u}_{b,i}\end{Bmatrix} \quad (i = 1,2,3,4) \tag{3.20}$$

where $\mathbf{N}(\xi_i)$ is ith substructure beam element shape function vector.

Substituting Equations (3.18)-(3.20) into Equation (3.17), coupling Equations (3.17) and (3.3) with Equation (3.16) and writing them as a single equation gives the governing equation of the coupled system as

$$\tilde{\mathbf{G}}\tilde{\mathbf{u}} = \tilde{\mathbf{F}} \tag{3.21}$$

where

$$\tilde{\mathbf{u}} = \{\mathbf{u}_v^{\mathrm{T}} \quad \mathbf{b}_1^{\mathrm{T}} \quad \mathbf{a}_1^{\mathrm{T}} \quad \mathbf{b}_2^{\mathrm{T}} \quad \mathbf{a}_2^{\mathrm{T}} \quad \mathbf{b}_3^{\mathrm{T}} \quad \mathbf{a}_3^{\mathrm{T}} \quad \mathbf{b}_4^{\mathrm{T}} \quad \mathbf{a}_4^{\mathrm{T}}\}$$

$$\tilde{\mathbf{F}} = \{\mathbf{0}_{6\times1}, r_1, r_2, r_3, r_4, \mathbf{N}^{\mathrm{T}}(\xi_1)r_1, \mathbf{N}^{\mathrm{T}}(\xi_2)r_2, \mathbf{N}^{\mathrm{T}}(\xi_3)r_3, \mathbf{N}^{\mathrm{T}}(\xi_4)r_4\}^{\mathrm{T}}$$

The specific components of $\tilde{\mathbf{G}}$ are given as

$$\tilde{\mathbf{G}} = \tilde{\mathbf{G}}_1 + \tilde{\mathbf{G}}_2$$

where

$$\widetilde{\mathbf{G}}_1 = \mathrm{diag}(\mathbf{G}_v, \mathbf{G}_t, \mathbf{G}_t, \mathbf{G}_t), \qquad \mathbf{G}_v = \mathbf{K}_v + \mathrm{i}\omega\mathbf{C}_v - \omega^2\mathbf{M}_v$$

$$\widetilde{\mathbf{G}}_2 = \begin{bmatrix} \mathbf{0}_{6\times1} & \mathbf{0} & \mathbf{0} \\ \mathbf{0} & -\mathbf{I}_{4\times4} & -\widetilde{\mathbf{N}}^{\mathrm{T}}\mathbf{W} \\ \mathbf{0} & -\mathbf{N} & \widetilde{\mathbf{N}}\widetilde{\mathbf{N}}^{\mathrm{T}}\mathbf{W} \end{bmatrix}, \quad \mathbf{G}_t = \begin{bmatrix} (\mathbf{G}_{aa} + \mathbf{P}_\beta)\mathbf{X}_b & \mathbf{G}_{ab}\mathbf{X}_a \\ \mathbf{G}_{ba}\mathbf{X}_b & (\mathbf{G}_{\boldsymbol{bb}} + \mathbf{P}_\alpha)\mathbf{X}_a \end{bmatrix}$$

$$\widetilde{\mathbf{N}} = \mathrm{diag}\big(\mathbf{N}(\xi_1), \mathbf{N}(\xi_2), \mathbf{N}(\xi_3), \mathbf{N}(\xi_4)\big)$$

and

$$\left(\mathbf{w}^{ii} = \begin{bmatrix} \mathbf{X}_b & \mathbf{0} \\ \mathbf{0} & \mathbf{X}_a \end{bmatrix}; \; i = 1,2,3,4\right); \left(\mathbf{w}^{ij} = \begin{bmatrix} \mathbf{X}_b\boldsymbol{\mu}^{(k_j-k_i)} & \mathbf{0} \\ \mathbf{X}_b\boldsymbol{\mu}^{(k_j-k_i-1)} & \mathbf{0} \end{bmatrix}; \; 1 \le i \le j \le 4\right); \left(\mathbf{w}^{ij} = \begin{bmatrix} \mathbf{0} & \mathbf{X}_a\boldsymbol{\mu}^{(k_i-k_j-1)} \\ \mathbf{0} & \mathbf{X}_a\boldsymbol{\mu}^{(k_i-k_j)} \end{bmatrix}; \; 1 \le j \le i \le 4\right)$$

4 Random vibration analysis of the uncertain coupled vehicle-track system

Equation (3.21) is the deterministic pseudo governing equation of the coupled vehicle-track system which is established by combining PEM and the symplectic method. In this section, the uncertain parameters are described by a specific PDF, the pseudo response is expanded in polynomial space, and finally the stochastic governing equation is solved by the Galerkin method.

4.1 Probabilistic description of the uncertain parameters

For the vehicle model, it is natural to assume that the uncertain kinetic parameters are random variables obeying some probability distribution. Normal or uniform distributions are commonly used. However, normal distributions of random variables may lead to negative infinite values, which can be meaningless for a physical problem, *e.g.* negative stiffness is not permissible. It is therefore necessary for the system parameters to be bounded. The value of uniform distribution variables is from -1 to 1, which does not cause instability. However for the current problem the system parameters should obey a more concentrated bounded distribution. Therefore, the Wigner semicircle distribution is adopted.

Denote the random parameter α by

$$\alpha = \bar{\alpha} + \tilde{\alpha} \tag{4.1}$$

where $\bar{\alpha}$ is a deterministic constant and $\tilde{\alpha}$ is a random variable obeying the Wigner semicircle distribution supported on interval $[-\kappa, \kappa]$ whose probability density function is

$$p(\tilde{\alpha}) = \begin{cases} \frac{2}{\pi\kappa^2}(\kappa^2 - \tilde{\alpha}^2)^{1/2} & |\tilde{\alpha}| \le \kappa \\ 0 & |\tilde{\alpha}| > \kappa \end{cases} \tag{4.2}$$

Calculate the mean and variance of α as

$$\mathrm{E}[\alpha] = \mathrm{E}[\bar{\alpha} + \tilde{\alpha}] = \bar{\alpha} \tag{4.3}$$

$$\mathrm{D}[\alpha] = \mathrm{E}[(\alpha - \bar{\alpha})^2] = \kappa^2/4 \tag{4.4}$$

where $\mathrm{E}[\cdot]$ is the expectation operator.

4.2 Pseudo excitation for the track irregularity

Actual track irregularity is a non-ideal smoothness characteristic of the rail surface caused by many random factors, such as manufacturing and abrasion. For the assumed randomness, the same class of track will have the same probability characteristic everywhere. Hence when a train runs along the track at uniform velocity, the excitation caused by the track irregularity can be regarded

as a stationary random process (Garg, 1984; Iwnicki, 2006). It is assumed that the track irregularity $r(x)$ with respect to the space coordinate x is a zero-mean stationary random process with power spectral density function $S_{rr}(\Omega)$.

Assume that the wheel is in contact with the rail at all times, *i.e.* there is no sliding or derailment. The track irregularity can be converted from the space domain $r(x)$ to the time domain $r(t)$ by the relationship $x = vt$. This gives a zero-mean stationary random process with respect to the time coordinate t, with the power spectral density function $S_{rr}(\omega)$ obtained from $S_{rr}(\Omega)$ as

$$S_{rr}(\omega) = (S_{rr}(\Omega))/v, \qquad \omega = \Omega v = 2\pi v/\lambda \tag{4.5}$$

where λ is the spatial wavelength.

The coupled system is subjected to four excitations at the wheel-rail contact points which are all from the same source. This fully coherent (multi-phase) random excitation can be regarded as a generalized single excitation. The pseudo excitation is constructed as

$$\tilde{\mathbf{F}} = \{\mathbf{0}_{6\times1}, e^{-\mathrm{i}\omega t_1}, e^{-\mathrm{i}\omega t_2}, e^{-\mathrm{i}\omega t_3}, e^{-\mathrm{i}\omega t_4}, \mathbf{N}^{\mathrm{T}}(\xi_1)e^{-\mathrm{i}\omega t_1}, \ldots \\ \mathbf{N}^{\mathrm{T}}(\xi_2)e^{-\mathrm{i}\omega t_2}, \mathbf{N}^{\mathrm{T}}(\xi_3)e^{-\mathrm{i}\omega t_3}, \mathbf{N}^{\mathrm{T}}(\xi_4)e^{-\mathrm{i}\omega t_4}\}^{\mathrm{T}}\sqrt{S_{rr}(\omega)}e^{\mathrm{i}\omega t} \tag{4.6}$$

Without loss of generality, it is assumed that t_1=0, so that t_i $(i = 2,3,4)$ is the time lag between the other excitations and the first excitation.

4.3 Solution of the stochastic governing equation

The stochastic governing equation in frequency domain can be expressed as

$$\tilde{\mathbf{G}}(\boldsymbol{\alpha})\tilde{\mathbf{u}} = \tilde{\mathbf{F}} \tag{4.7}$$

where

$$\tilde{\mathbf{G}}(\boldsymbol{\alpha}) = \bar{\mathbf{G}}_0 + \Sigma_{i=1}^{n}\tilde{\alpha}_i\tilde{\mathbf{G}}_i$$

$\bar{\mathbf{G}}_0$ and $\tilde{\mathbf{G}}_i$ $(i = 1,2,\ldots,n)$ are the mean value matrix and the nominal variance matrix, respectively, which are constructed in Equation (3.21); $\tilde{\alpha}_i$ are independence random variables denoted by Equation (4.1) which are the components of the vector $\boldsymbol{\alpha}$.

4.3.1 Polynomial chaos expansion

If we can obtain the pseudo response $\tilde{\mathbf{u}}$, the response PSD can be obtained efficiently from Equation (2.8). In this section, the pseudo response is expanded in polynomial space to assess the uncertainty impact on the power spectrum and spectral moments.

From the viewpoint of functional analysis, the dynamic responses of random structures can be regarded as the locus of solutions in the function spaces. By selecting the appropriate basis function$\{\varphi_l(\boldsymbol{\alpha})\}_{l=0}^{\infty}$, the random response $\tilde{\mathbf{u}}(\boldsymbol{\alpha}, t)$ in Equation (4.7) can be expanded as

$$\tilde{\mathbf{u}}(\boldsymbol{\alpha}, t) = \Sigma_{l=1}^{\infty}\mathbf{x}_l\varphi_l(\boldsymbol{\alpha})e^{\mathrm{i}\omega t} \tag{4.8}$$

where $\mathbf{x}_l$ is the deterministic coefficient vector, which can be understood as the projection of $\tilde{\mathbf{u}}$ on the basis functions .

Consider now the orthogonal polynomials as basis functions:

$$\varphi_l(\boldsymbol{\alpha}) = \prod_{i=1}^{n} P_{l_i}(\tilde{\alpha}_i) \tag{4.9}$$

where, $P_{l_i}(\alpha_i)$ is the l_ith orthogonal polynomial of the random variable α_i. Hypothetically there are n independent random variables and each one has an m_i-order orthogonal expansion, with $0 \le l_i \le m_i, 1 \le l \le L$ and with $L = \prod_{i=1}^{n}(m_i + 1)$ as the number of polynomial basis functions.

The choice of orthogonal polynomials depends on the probability distribution of the random variables, *e.g.* Hermite polynomials for standard normal distribution and Legendre polynomials

for uniform distribution. In this work, Chebyshev polynomials (Borwein and Erdēlyi, 1995) are adopted, whose expression is

$$H_n(\tilde{\alpha}) = \sum_{k=0}^{[n/2]} \frac{(-1)^k (n-k)!}{k!(n-2k)!} (2\tilde{\alpha})^{n-2k} \tag{4.10}$$

e.g. the first three are:

$$H_0(\tilde{\alpha}) = 1, H_1(\tilde{\alpha}) = 2\tilde{\alpha}, H_2(\tilde{\alpha}) = 4\tilde{\alpha}^2 - 1, H_3(\tilde{\alpha}) = 8\tilde{\alpha}^3 - 4\tilde{\alpha} \tag{4.11}$$

The weight function of the Chebyshev polynomials is $2/\pi\sqrt{1-\tilde{\alpha}^2}$. This connects the expectation of the random variable from Equation (4.2) and the orthogonality of the polynomials giving:

Orthogonality: $$\int_{-1}^{1} 2/\pi\sqrt{1-\tilde{\alpha}^2} H_m(\tilde{\alpha}) H_n(\tilde{\alpha}) d\tilde{\alpha} = \delta_{mn} \tag{4.12}$$

Recursiveness: $$\tilde{\alpha} H_n(\tilde{\alpha}) = \frac{1}{2}[H_{n-1}(\tilde{\alpha}) + H_{n+1}(\tilde{\alpha})] \tag{4.13}$$

According to Equations (4.8) and (4.9), $\tilde{\mathbf{u}}(\boldsymbol{\alpha}, t)$ can be expanded on the Chebyshev polynomials basis function with an appropriate truncation

$$\tilde{\mathbf{u}}(\boldsymbol{\alpha}, t) = \left(\sum_{0 \le l_j \le m_j}^{L} \mathbf{x}_{l_1 l_2 \ldots l_n} \prod_{j=1}^{n} H_{l_j}(\tilde{\alpha}_j) \right) e^{\mathrm{i}\omega t} \tag{4.14}$$

which can be re-written in the following matrix form to facilitate derivation

$$\tilde{\mathbf{u}}(\boldsymbol{\alpha}, t) = \boldsymbol{\Phi}(\boldsymbol{\alpha}) \mathbf{x} e^{\mathrm{i}\omega t} \tag{4.15}$$

where $\boldsymbol{\Phi}(\boldsymbol{\alpha})$ is a block diagonal matrix with each diagonal element being $\boldsymbol{\varphi}(\boldsymbol{\alpha}) = [\prod_{i=1}^{n} H_0(\tilde{\alpha}_i), \ldots, \prod_{i=1}^{n} H_m(\tilde{\alpha}_i)]_{1\times L}$ and $\mathbf{x}$ is a column vector. Equation (4.15) is a pseudo response polynomial chaos expansion model. If the deterministic coefficient vector $\mathbf{x}$ is known, the quantitative assessment of the uncertain impact is achieved by using statistical theory.

4.3.2 Galerkin method

Assume now that the external loads are independent of the vehicle-track system. Substituting Equation (4.15) into Equation (4.7), left multiplying by $\boldsymbol{\Phi}(\boldsymbol{\alpha})^{\mathrm{T}}$ on both sides and calculating the expectation to $\boldsymbol{\alpha}$, the governing equation for random response prediction is obtained, according to Equations (4.12) and (4.13), as

$$\mathbf{A}_{\tilde{G}} \mathbf{x} = \mathbf{b}_{\tilde{F}} \tag{4.16}$$

In order to explain the specific forms of $\mathbf{A}_{\tilde{G}}$ and $\mathbf{b}_{\tilde{F}}$, $\otimes$ is used to denote the Kronecker-product and the three matrices $\mathbf{T}$, $\mathbf{U}$ and $\mathbf{E}$ are defined as

$$\mathbf{T}_i = \begin{bmatrix} 1 & & & \\ & 1 & & \\ & & \ddots & \\ & & & 1 \end{bmatrix}_{(m_i+1)\times(m_i+1)} \quad \mathbf{U}_i = \begin{bmatrix} 0 & 0.5 & & \\ 0.5 & 0 & \ddots & \\ & \ddots & \ddots & 0.5 \\ & & 0.5 & 0 \end{bmatrix}_{(m_i+1)\times(m_i+1)} \quad \mathbf{E} = \begin{bmatrix} 1 \\ 0 \\ \vdots \\ 0 \end{bmatrix}_{L\times 1}$$

Hence

$$\mathbf{A}_{\tilde{G}} = \mathbf{A}_{\tilde{G}_0} + \sum_{i=1}^{n} \mathbf{A}_{\tilde{G}_i} \tag{4.17}$$

$$\mathbf{A}_{\tilde{G}_0} = \overline{\mathbf{G}}_0 \otimes (\mathbf{T}_1 \otimes \mathbf{T}_2 \otimes \cdots \otimes \mathbf{T}_n)$$

$$\mathbf{A}_{\tilde{G}_i} = \widetilde{\mathbf{G}}_i \otimes (\mathbf{T}_1 \otimes \mathbf{T}_2 \otimes \cdots \mathbf{U}_i \otimes \cdots \otimes \mathbf{T}_n)$$

and

$$\mathbf{b}_{\tilde{F}} = \tilde{\mathbf{F}} \otimes \mathbf{E} \tag{4.18}$$

The governing equation given in Equation (4.7) has thus been transformed into the high-order deterministic equation given by Equation (4.16), which is easy to solve. When the component column vector $\mathbf{x}$ has been obtained, the response $\tilde{\mathbf{u}}(\boldsymbol{\alpha}, t)$ can be calculated from Equation (4.15). It is obvious that the coefficient matrix of the governing equation Equation (4.16) is sparse, which

yields computational savings.

4.3.3 Statistical assessment

Assume that a specified response is concerned and expand it as

$$\tilde{u}(\boldsymbol{\alpha},t)=\boldsymbol{\varphi}(\boldsymbol{\alpha})\hat{\mathbf{x}}e^{\mathrm{i}\omega t}=\Sigma_{l=1}^{L}\varphi_l(\boldsymbol{\alpha})\hat{x}_l e^{\mathrm{i}\omega t} \tag{4.19}$$

where $\hat{\mathbf{x}}$ is the projection of the specified response on the basis functions, and is part of the $\mathbf{x}$ given by Equation (4.16).

The PSD and variance can easily be obtained by using PEM, giving

$$S_{out}(\boldsymbol{\alpha},\omega)=\left(\tilde{u}(\boldsymbol{\alpha},t)\right)^{*}\left(\tilde{u}(\boldsymbol{\alpha},t)\right)^{\mathrm{T}}=\boldsymbol{\varphi}(\boldsymbol{\alpha})\hat{\mathbf{x}}^{*}\hat{\mathbf{x}}^{\mathrm{T}}\boldsymbol{\varphi}(\boldsymbol{\alpha}) \tag{4.20}$$

$$\sigma_{out}^2(\boldsymbol{\alpha})=2\int_0^{+\infty}S_{out}(\boldsymbol{\alpha},\omega)d\omega \tag{4.21}$$

The mean of the random vibration power spectrum caused by the uncertain parameters can found by taking the expectation on Equation (4.20), by using the orthogonality of the polynomials, as

$$\bar{S}_{out}=\mathrm{E}[S_{out}(\boldsymbol{\alpha},\omega)]=\mathrm{E}[\boldsymbol{\varphi}(\boldsymbol{\alpha})\hat{\mathbf{x}}^{*}\hat{\mathbf{x}}^{\mathrm{T}}\boldsymbol{\varphi}^{\mathrm{T}}(\boldsymbol{\alpha})]=\Sigma_{l=1}^{L}|\hat{x}_l|^2 \tag{4.22}$$

where $|\cdot|$ is the modulo operation. Equation (4.22) shows that the mean of the response PSD of concern can be obtained by summing up the squares of the modulo of each coefficient, which yields both very concise expressions and efficient computation.

The mean of the response variance of concern is found by

$$\bar{\sigma}_{out}^2=\mathrm{E}[\sigma_{out}^2(\boldsymbol{\alpha})]=2\int_0^{+\infty}\bar{S}_{out}d\omega \tag{4.23}$$

Also, the variance of the response PSD or the variance of concern is found by

$$\mathrm{D}[S_{out}(\boldsymbol{\alpha},\omega)]=\mathrm{E}[(S_{out}-\bar{S}_{out})^2] \tag{4.24}$$

$$\mathrm{D}[\bar{\sigma}_{out}^2(\boldsymbol{\alpha},\omega)]=\mathrm{E}[(\sigma_{out}^2-\bar{\sigma}_{out}^2)^2] \tag{4.25}$$

When there are many variables, a multi-dimensional integral operation is needed to calculate the variance of random vibration response caused by uncertain parameters directly from Equations (4.24) and (4.25). Unfortunately, unlike for the expectation operation, the variance operation cannot use the orthogonality of the basis functions. Therefore Monte Carlo method integration is recommended here because, due to the simple form of the statistical functions, it is highly efficient.

5 Numerical examples

Vehicle parameters			
Carriage mass M_c	34×10^3kg	Primary damping c_t	12×10^3Ns/m
Carriage inertia J_c	2.277×10^6m^4	Secondary stiffness k_c	800×10^3N/m
Bogie mass M_t	3000kg	Secondary damping c_c	160×10^3Ns/m
Bogie inertia J_t	2710m^4	Wheel spacing $2l_t$	2.4m
Wheel mass M_w	1400kg	Bogie spacing $2l_c$	18m
Primary stiffness k_t	1100×10^3N/m	Contact constant G	5.135×10^{-8}m/N$^{2/3}$
Track parameters			
Rail bending rigidity EI	13.25×10^6Nm^2	Ballast stiffness k_b	4.8×10^8N/m

Rail linear density m_r	121.28kg/m	Subgrade stiffness k_f	13×10^7N/m
Sleeper spacing L	0.545m	Rail pad damping c_p	7.5×10^4Ns/m
Sleeper mass m_s	237kg	Ballast damping c_b	5.88×10^4Ns/m
Ballast mass m_b	1365.2kg	Subgrade damping c_f	3.115×10^4Ns/m
Rail pad stiffness k_p	15.6×10^7N/m		

Table 1The parameters of vehicle and track

The parameters of the coupled vehicle-track system were given the values shown in Table 1 (Zhang *et al*., 2010) and the uncertain parameters are shown in Table 2. From front to rear, there are five locations, head (I), front spring (II), center (III), rear spring (IV) and stern (V) under consideration as shown in Figure 1. The PSD of the track irregularity is expressed as:

$$S_r(\Omega) = \begin{cases} \frac{0.25\times0.0339\times0.8245^2}{\Omega^2(\Omega^2-0.8245^2)} \ (cm^2/rad/m) & \text{when } \Omega \le 2\pi \\ 0.036(\Omega/2\pi)^{-3.15} \ (mm^2/rad/m) & \text{when } \Omega > 2\pi \end{cases} \tag{5.1}$$

where Ω is the space circular frequency. The power spectral density function in the time domain was transformed from $S_r(\Omega)$ by Equation (4.5).

Parameter α	**Mean** $\bar{\alpha}$	**Standard deviation** $\kappa/2$
Primary stiffness k_t	1100×10^3N/m	220×10^3N/m
Primary damping c_t	12×10^3Ns/m	2.4×10^3Ns/m
Secondary stiffness k_c	800×10^3N/m	160×10^3N/m
Secondary damping c_c	160×10^3Ns/m	32×10^3Ns/m
Carriage mass M_c	34×10^3kg	6.8×10^3kg
Carriage inertia J_c	2.277×10^6m^4	4.554×10^5m^4

Table 2 Uncertain parameters

5.1 The kinetic parameter sensitivity analysis of the vehicle system

For different kinetic parameters, impacts on any specified response of concern are different. It is a waste of computing cost to account for all uncertainty of the parameters. So firstly, the important uncertain parameters were found using response sensitivity analysis as a filter. For the sensitivity of the vertical acceleration PSD to the connection parameters, the differential sensitivity method was adopted as Equation (5.2)

$$\varepsilon_i = \frac{\Delta S_{out}(\alpha_i,\omega)}{\Delta\alpha_i}, \ i = 1,2,\dots,n \tag{5.2}$$

The differential step used was 0.001 times the mean value. The sensitivities of the vehicle body acceleration PSD to the primary and secondary stiffness and damping were calculated. The nondimensionalized sensitivities are shown in Figure 3. It can be seen that the sensitivity curves change with frequency. The sensitivities can be positive or negative, so that the influence of the response may be increased or reduced. Figure 3 shows that the system is most sensitive to secondary damping c_c^i and primary stiffness k_t^i, and so in the following the focus is on their uncertainty propagation.

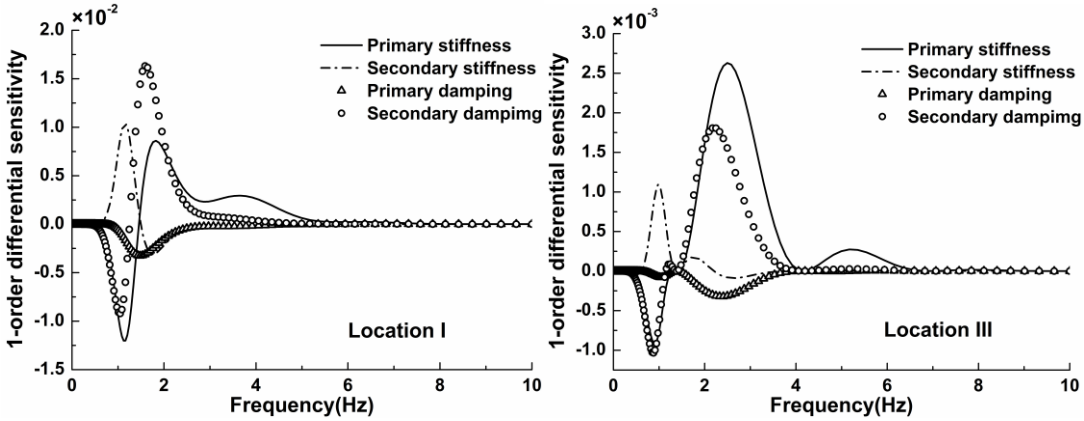

Figure 3. 1-order differential sensitivities of acceleration PSD to the connection parameters for locations I and III.

5.2 Quantitative analysis of impact on vehicle body vibration of different uncertain parameters

Assume that the uncertain parameter probabilities can be described by Equation (4.1). The vehicle body acceleration PSDs given by the proposed method are shown in Figure 4 for $\kappa/\bar{\alpha} = 0.4$ and a velocity of 180km/h. Figure 4 (a) shows the mean, standard deviation (SD) and coefficient of variance (CV) of the vertical acceleration PSD of location I when secondary damping c_c^i is uncertain, whereas Figure 4 (b) gives the mean, SD and CV of the vertical acceleration PSD of location III when primary stiffness k_t^i is uncertain. Hence it can be seen that the uncertainties of the connection parameters do not change the position of the peak of acceleration PSD but they do change its amplitude. In addition, the mean of the uncertain system PSD may be higher or lower than for the deterministic system. Sensitivity analysis is only able to achieve a qualitative description and quantitative analysis should be carried out for the specific impact. In Figure 4 (b3), the four highest peaks of the CV curve occur at the same frequencies of the valleys with the mean values close to zero in Figure 4 (b1). Such peaks caused by the denominators (mean values) close to zero are of little significance. In this case we prefer SD to CV to measure the deviation of the PSD response. In Figure 4 (a), however, the peaks of mean, SD and CV take place at the same frequency, which means the dimensionless measure of CV should be a better choice for the measure of the PSD response deviation.

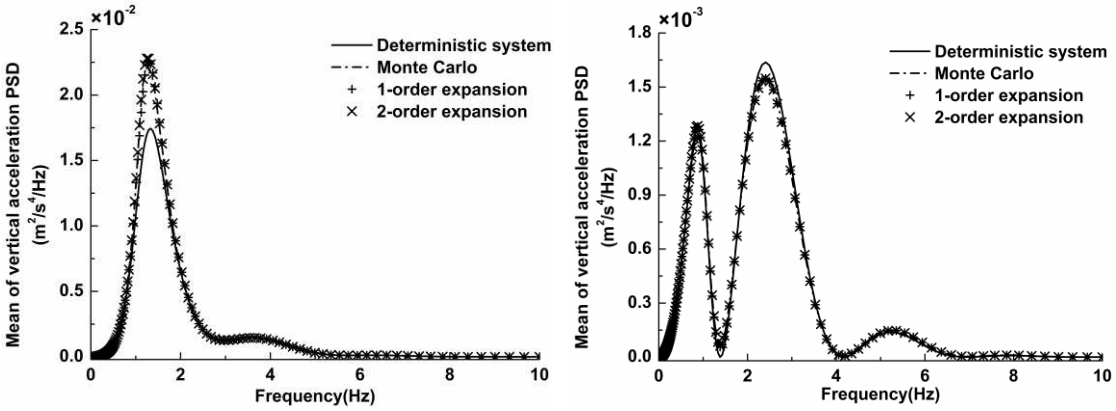

(a1) (b1)

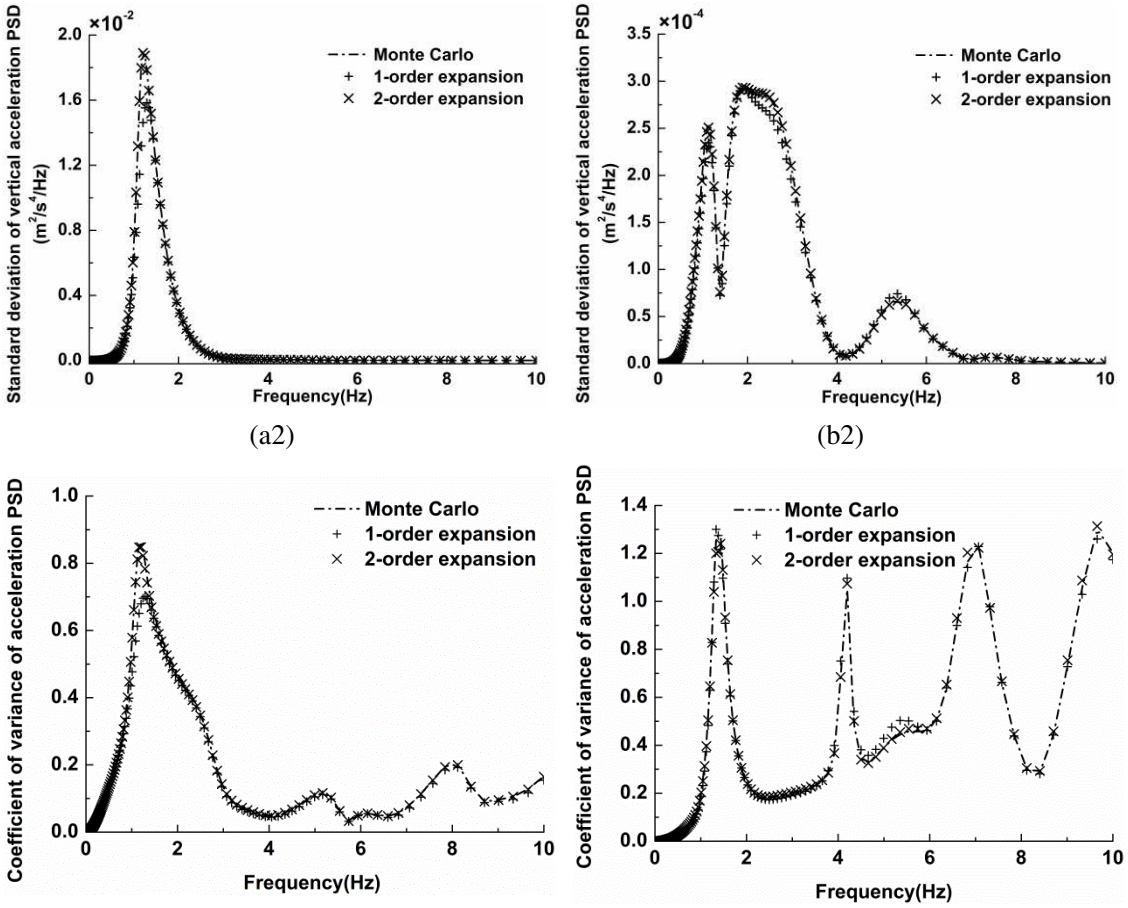

Figure 4. Mean, SD and CV of acceleration PSD for (a) location I when c_c^i is uncertain and (b) location III when k_t^i is uncertain.

On the other hand, the impacts of uncertain inertia parameters of the system on the vibration were also investigated. It turns out that the impact of inertia parameter uncertainty to vibration response is largely local, *i.e.* it affects the corresponding degree of freedom, but has little effect on others. Only the vehicle body response is of concern, so considering the uncertainty of the inertia parameters of the vehicle body, *i.e.* M_c and J_c, the mean, SD and CV of the vertical acceleration PSD of location III are given in Figure 5, which shows that the uncertainty of the vehicle body inertia parameter has a great influence on the acceleration PSD at location III, exceeding that of uncertainty of k_t^i.

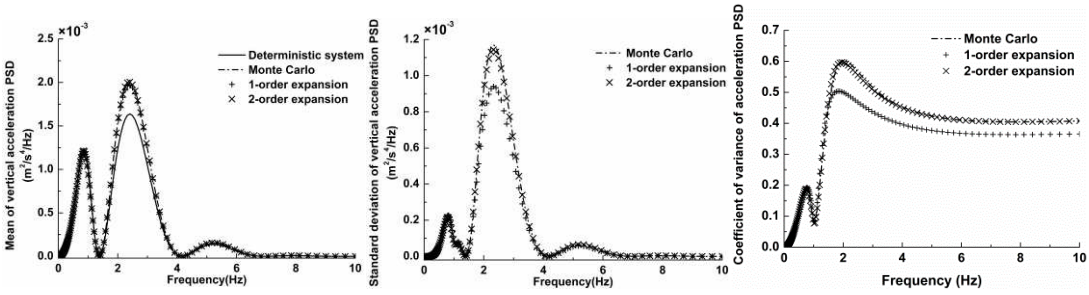

Figure 5. Mean, SD and CV of acceleration PSD for location III when M_c and J_c are uncertain.

To verify the correctness of the proposed method, comparison is made with direct Monte Carlo

results. Figure 4 and 5 show the results of direct Monte Carlo simulation using 1000 samples, including the statistical analysis of the first two order moments. It can be seen that the 1-order moment can agree well when the random variables take the 1-order orthogonal expansion; meanwhile, 2-order orthogonal expansion can satisfy the accuracy of 2-order moment. It turns out that the 2-order expansion agrees well with Monte Carlo simulation even when the peak of CV of response is close to 1. Monte Carlo simulation needs to establish and solve the equation repeatedly. To ensure accuracy, the sample size is considerable, so that it is very time consuming. Instead the proposed method expands the pseudo response in polynomial space. The original random system dynamics equation converts into the expanded deterministic equation by using the orthogonality and recursiveness of the polynomials. The projection in polynomial space is obtained by solving the expanded deterministic equation only once, then the uncertain response is quantified by using the effective uncertainty polynomial chaos expansion prediction model, see Equation (4.19). The CPU times of the two methods are compared in Table 3 to show that the proposed method is much more efficient than Monte Carlo simulation.

k_t^i uncertain (4 variables)			c_c^i uncertain (2variables)		
Monte Carlo	1-order	2-order	Monte Carlo	1-order	2-order
538.16s	4.68s	23.39s	554.29s	1.46s	2.36s

Table 3 Comparison of CPU time between methods

5.3 Random vibration analysis of uncertain coupled system at different velocities

The velocity v of the train is an important factor which influences the coupled system response and so the results given in Figure 6 were obtained by using the hybrid pseudo excitation polynomial chaos expansion (PEM-PCE) method for velocities of 180km/h, 240km/h and 300km/h. Combined with the discussion in the previous section, it can be seen that c_c^i, k_t^i, M_c and J_c are important when calculating the response of the uncertain coupled vehicle-rack system under the track irregularity. Figure 6 shows the mean and SD of the acceleration PSD for locations I and III for different velocities. It can be seen that when the velocity increases, the peak and shape of the PSD curve are changed. This is mainly due to the phase lag between the four wheels changing significantly as the velocity increases. It can also be seen that the difference between the mean of uncertain response and the deterministic system response is approximately independent of velocity. This can be explained by the fact that the system parameter uncertainty and the track irregularity random excitation are independent.

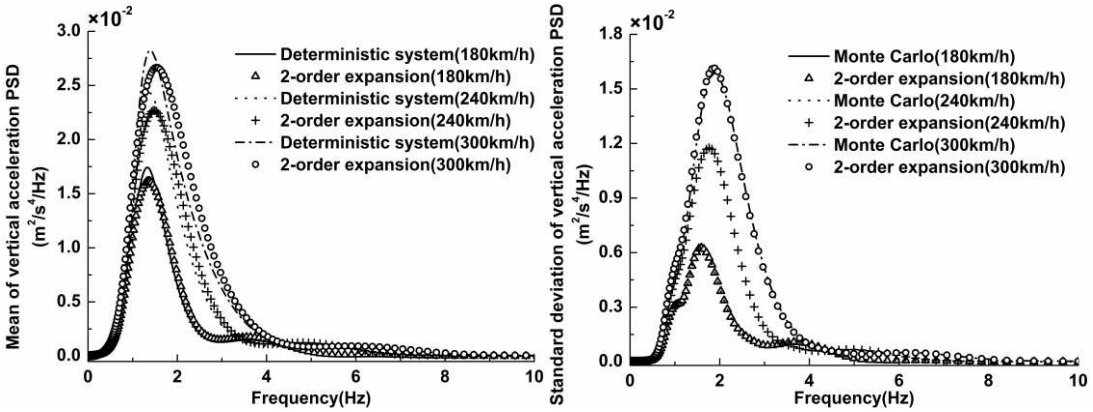

(a)

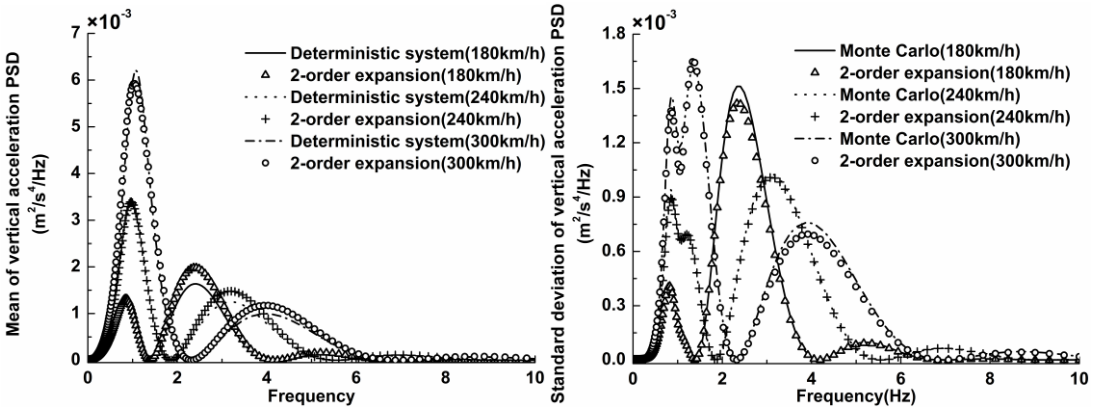

(b)

Figure 6. Mean and SD of acceleration PSD for (a) location I and (b) location III for different velocities when k_t^i, c_c^i, M_c and J_c are all uncertain.

5.4 Impact of uncertain parameter on the stability index

According to the aforementioned analysis for random vibration responses with respect to the uncertain parameters, it can be seen that secondary damping c_c^i, primary stiffness k_t^i and the vehicle body inertias M_c and J_c are the most important parameters for the random vibration analysis of the uncertain system. Therefore, we must consider these uncertain parameters in combination in analysis when assessing running stability. The Chinese Railway vehicle dynamic performance evaluation and test specification (GB5599-85, 1985) for evaluation of train running stability was selected. The corresponding index is

$$W = 7.08\left[\int_{0.5}^{80}\left(\frac{F(f)}{f}\right)^{\frac{2}{3}} G(f)df\right]^{3/20} \tag{5.3}$$

where $G(f)$ is the power spectral density of acceleration, f is the frequency in Hz and $F(f)$ is the frequency correction factor, with

$$F(f) = \begin{cases} 0.325f^2 & 0.5 \le f \le 5.9 \\ 400/f & 5.9 < f < 20 \\ 1 & f \ge 20 \end{cases} \tag{5.4}$$

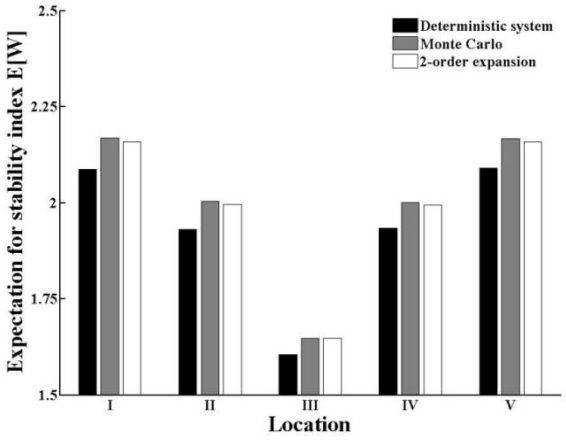

Figure 7. The mean of the stochastic stability index at different locations

Figure 7 shows the expectation for the stability index at different locations. Clearly the stability index at all locations is higher than predicted by the deterministic system and although they all achieve the standard (*i.e.* they are lower than 2.5), neglect of the parameter uncertainty will lead to potentially risky analysis results. In addition, comparing the stability index at different locations shows that it is lowest in the middle and highest at the ends. Locations I and III are respectively the worst and the optimum location for the stability index, as investigated below. The mean and variance of the stability at location I are 2.104 and 0.026, and at location III they are 1.624 and 0.011. The PDF of the random stability index was also investigated by taking the log likelihood function value as the standard and selecting the inverse Gaussian distribution to fit the PDF. This better reflects the overall probability characteristics, as shown in Figure 8. Further analysis showed that the stability index at location I has a 98.94% probability of being less than 2.5, and the stability index at location III has a 94.89% probability of being less than 1.8. The probability distribution of the stability index provides a good indicator when performing reliability analysis.

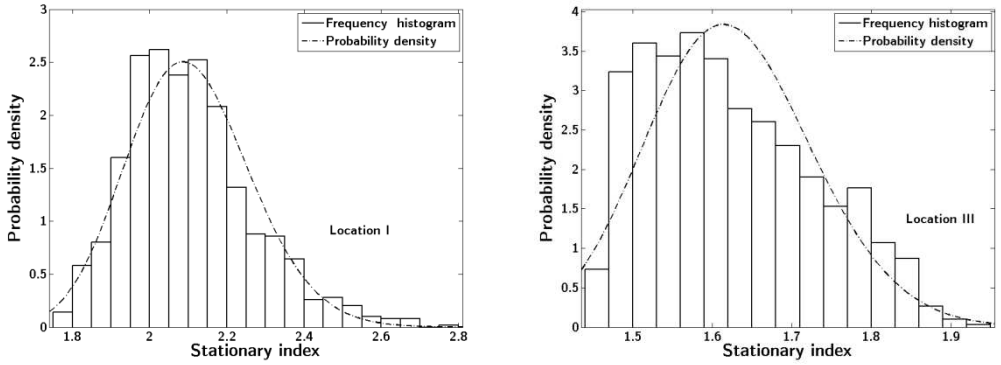

Figure 8. Probability density fitting of the stability index at locations I and III.

6 Conclusions

A new effective assessment method has been developed for random vibration of an uncertain coupled vehicle-track system under track irregularity. The dynamic equation of coupled vehicle-track systems under mixed physical coordinates and dual coordinates has been established in the framework of the Hamiltonian system, and the governing equation with respect to the uncertain parameters has been derived by using orthogonal polynomials for the dynamic analysis of coupled systems. An assessment of random vibration with respect to the uncertain parameters has been established for the coupled vehicle-track system by using the pseudo-excitation method. Numerical results show that the established method has high accuracy and that this work provides an effective means for solving practical engineering problems that involve the uncertainty of vehicle-track systems.

References

Borwein, P.B. and Erdēlyi, T. (1995), Polynomials and Polynomial Inequalities. Springer , New York.

Cameron, R.H. and Martin, W.T. (1947), "The orthogonal development of non-linear functionals in series of Fourier-Hermite functionals", *Annals of Mathematics*, Vol. 48, pp. 385-92.

Caprani C.C. (2014), "Application of the pseudo-excitation method to assessment of walking variability on footbridge vibration", *Computers & Structures*, Vol. 132, pp. 43-54.

Chang, T.P., Lin, G.L. and Chang, E. (2006), "Vibration analysis of a beam with an internal hinge subjected to a random moving oscillator", *International Journal of Solids and Structures*, Vol.43, pp. 6398-412.

Clough, R.W. and Penzien, J. (1975), Dynamics of Structures, McGraw-Hill, New York.

D'Aveni, A., Muscolino, G. and Ricciardi, G. (1996), "Stochastic analysis of a simply supported beam with uncertain parameters subjected to a moving load", Structural Dynamics: EURODYN'96, Florence, Italy: 439-46.

De Rosa, S., Franco F. and Ciappi E. (2015), "A simplified method for the analysis of the stochastic response in discrete coordinates", *Journal of Sound and Vibration*, Vol. 339: pp. 359-75.

Garg, V.K. and Dukkipati, R.V. (1984), Dynamics of Railway Vehicle Systems, Academic Press , New York.

GB5599-1985: Railway vehicle-Specification for evaluation the dynamic performance and accreditation test. 2-3.

Ghanem, R.G. and Kruger, R.M. (1996), "Numerical solution of spectral stochastic finite element systems", *Computer Methods in Applied Mechanics and Engineering*, Vol.129, pp. 289-303.

Ghanem, R.G. and Red-Horse, J. (1999), "Propagation of probabilistic uncertainty in complex physical systems using a stochastic finite element approach", *Physica D: Nonlinear Phenomena*, Vol. 133, pp. 137-44.

Ghanem, R.G. and Spanos, P.D. (1991), Stochastic finite elements: a spectral approach, Springer-Verlag, New York.

Gładysz, M. and Śniady, P. (2009), "Spectral density of the bridge beam response with uncertain parameters under a random train of moving forces", *Archives of Civil and Mechanical Engineering*, Vol. 9, pp.31-47.

Iwnicki, S. (2006), Handbook of Railway Vehicle Dynamics, CRC Press, Boca Raton.

Kewlani, G., Crawford, J. and Iagnemma, K. (2012), "A polynomial chaos approach to the analysis of vehicle dynamics under uncertainty", *Vehicle System Dynamics*, Vol. 50, pp. 749-74.

Lin, J.H. (1992), "A fast CQC algorithm of PSD matrices for random seismic responses", *Computers and Structure*, Vol. 44, pp. 683-87.

Lin, J.H., Fan, Y., Bennett, P.N. and Williams, F.W. (1995), "Propagation of stationary random waves along substructural chains", *Journal of Sound and Vibration*, Vol. 180, pp. 757-67.

Lin, J.H., Zhang Y.H. and Zhao Y. (2011), "Pseudo excitation method and some recent developments", *Procedia Engineering*, Vol. 14, pp. 2453-8.

Lin J.H., Zhang Y.H. and Zhao Y. (2014), "Seismic random response analysis", Chen W.F. and Duan L.(Ed.), Bridge Engineering Handbook, CRC Press, Boca Raton, pp. 133-62.

Lin, J.H., Zhao, Y. and Zhang, Y.H. (2001), "Accurate and highly efficient algorithms for structural stationary/non-stationary random responses", *Computer Methods in Applied Mechanics and Engineering*, Vol. 191, pp. 103-11.

Muscolino, G., Benfratello, S. and Sidoti, A. (2002), "Dynamics analysis of distributed parameter system subjected to a moving oscillator with random mass, velocity and acceleration", *Probabilistic engineering mechanics*, Vol. 17, pp. 63-72.

Thompson, D.J. (1993), "Wheel-rail noise generation, part IV: contact zone and results", *Journal of Sound and Vibration*, Vol. 161, pp. 447-66.

Wiener, N. (1938), "The homogeneous chaos", *American Journal of Mathematics*, Vol. 60, pp. 897-936.

Wu, S.Q. and Law, S.S. (2010), "Dynamic analysis of bridge–vehicle system with uncertainties based on the finite element model", *Probabilistic Engineering Mechanics*, Vol. 25, pp. 425-32.

Wu, S.Q. and Law, S.S. (2011), "Dynamic analysis of bridge with non-Gaussian uncertainties under a moving vehicle", *Probabilistic Engineering Mechanics*, Vol. 26, pp. 281-93.

Xiu, D. (2010), Numerical Methods for Stochastic Computations: A Spectral Method Approach, Princeton University Press, Princeton.

Xiu, D. and Karniadakis, G.E. (2002), "The Wiener-Askey polynomial chaos for stochastic differential equations", *SIAM Journal on Scientific Computing*, Vol. 24, pp. 619-44.

Yu, L. (2010), Fatigue Reliability of Ship Structures, PhD thesis, University of Glasgow, Glasgow.

Zhang, W.S. and Xu Y.L. (1999), "Dynamic Characteristics and seismic response of adjacent buildings linked by discrete

dampers", *Earthquake Engineering and Structural Dynamics*, Vol. 28, pp. 1163-85.

Zhang, Y.W., Lin, J.H., Zhao, Y., Howson, W.P. and Williams, F.W. (2010), "Symplectic random vibration analysis of a vehicle moving on an infinitely long periodic track", *Journal of Sound and Vibration*, Vol. 329, pp. 4440-54.